

# Design of an orbit determination computer for AI autonomous navigation

Aurel Zeqaj<sup>1,a\*</sup>

<sup>1</sup>Dipartimento di Ingegneria Industriale, Alma Mater Studiorum – Università di Bologna, Forlì, Italy

<sup>a</sup>aurel.zeqaj2@unibo.it

**Keywords:** EKF, DeepNav, Navigation, Autonomous

**Abstract.** In the context of the growing demand for autonomous navigation solutions able to reduce the cost of a space mission, the DeepNav project, financed by ASI, has the objective to develop a navigation subsystem relaying solely on the use of onboard assets, e.g. optical images, artificial intelligence algorithms and an Extended Kalman Filter, to perform the navigation of a CubeSat around minor celestial bodies. This manuscript describes the work performed at University of Bologna in the context of the project, in particular for the development of an orbit determination computer, which uses an estimation filter to reconstruct the trajectory of the spacecraft taking as input the optical observables previously processed by the artificial intelligence algorithms.

## Introduction

In recent years, the use of micro- and nano-satellites for space exploration has increased rapidly, mainly due to the reduction in launch and space segment costs that this type of technology entails [1,2,3,4]. Unfortunately, this does not (at least for now) correspond to a reduction in the ground segment. For example, the current approach for deep space navigation is to use radiometric tracking, obtained from ground antennas [5,6], which is still very demanding in terms of human and technical resources. In that respect, autonomous navigation in the vicinity of a celestial body can benefit greatly from the application of artificial intelligence approaches.

The 'DeepNav' [7] project, financed by the Italian Space Agency (ASI) and developed by a consortium consisting of AIKO<sup>1</sup> (prime), Politecnico di Milano<sup>2</sup>, and Università di Bologna<sup>3</sup>, has the aim of designing and testing an innovative navigation technique based on images and the use of artificial intelligence algorithms, for the exploration of asteroids [8,9,10], without any dependence on the Earth ground segment.

In the following sections, the work performed at the University of Bologna on the navigation computer (Figure 1) will be described.

## Dynamical Model

For the final test campaign of the project, a set of case studies were designed, including circular and hyperbolic trajectories around the two targeted bodies, i.e. asteroids 101955 Bennu and 25143 Itokawa, varying the following characteristics:

- Radius at the pericenter;
- Inclination of the orbit;
- Rotation angle of the asteroids;

The dynamic model [11,12,13] was developed accordingly, taking into account contributions due to the following accelerations:

<sup>1</sup> <https://www.aikospace.com/>, last access: 08/03/2023

<sup>2</sup> <https://dart.polimi.it/>, last access: 08/03/2023

<sup>3</sup> <https://site.unibo.it/radioscience-and-planetary-exploration-lab/en>, last access 08/03/2023

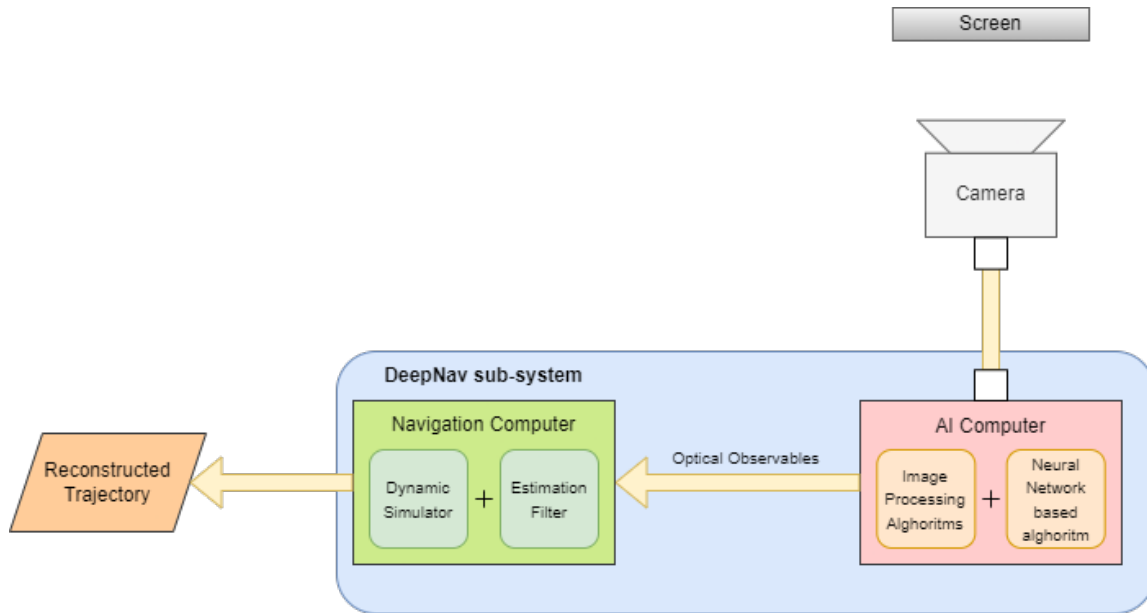


Figure 1: Structure of the DeepNav sub-system

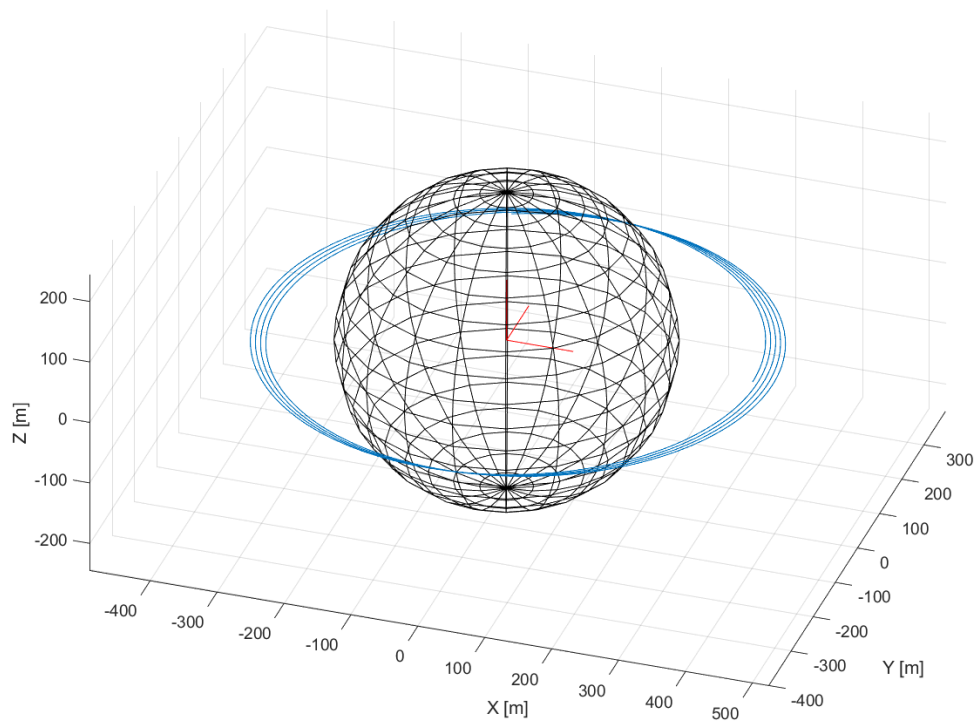


Figure 2: An example of simulator output. A quasi-circular orbit propagated using the point-mass model of the asteroid Bennu and the contribution due to the SRP. The S/C is at  $5/3$  of the mean radius of Bennu and at an inclination of  $0^\circ$ .

- Point-mass gravitational acceleration generated by the asteroids<sup>4</sup>;
- Third-body gravitational acceleration produced by the Sun and Jupiter<sup>5</sup>;
- Non-spherical gravitational acceleration, modeled using an expansion in spherical harmonics;
- Solar radiation pressure (SRP) acceleration using a simplified box-wing model made by a collection of flat plates.

Figure 2 shows an example of a quasi-circular orbit<sup>6</sup> of the DeepNav spacecraft around asteroid Bennu<sup>7</sup> obtained from the simulator, taking into consideration only the point-mass gravity and the SRP accelerations.

### Orbit Determination Filter

The filter developed for the simulator is an Extended Kalman Filter (EKF) [11,13] (Figure 3), which combines the a-priori information provided by the dynamic model with measurements from the AI computer (representing the position of the S/C obtained from the processed images of the camera) in a sub-optimal sequential algorithm. The non-optimality is given by the fact the Kalman filter is designed for linear systems that are only affected by Gaussian noise both in the process and the measurements, while the extension to non-linear system implies a certain degree of approximation, which in the case of EKF is a first-order approximation. In fact, the computation of the Kalman gain and the covariance matrix associated with the estimation is performed by linearizing the system around the last estimated state point. For weakly non-linear systems, such as the orbit model with time updates in the order of seconds, the use of EKF is fully justified, and no definitive evidence is given in the literature on the eventual benefits coming from different types of filters.

The equation that realizes the Kalman based estimation (the combination between a priori propagation and the measurements) is given by:

$$\hat{x}_k = \hat{x}_x^- + K_k(z_k - H_k\hat{x}_k^-). \tag{1}$$

Where  $\hat{x}_x^-$  is the a priori propagated state,  $K_k$  is the Kalman gain,  $z_k$  is the vector of measurements and  $H_k$  is the matrix that traduces the a priori state estimation into the related a priori measurement. The provided filter is based on a linear discrete system assumption with additive white Gaussian noise, which can be generally expressed as

$$x_{k+1} = \phi_k x_k + u_k. \tag{2}$$

$$z_k = H_k x_k + v_k \tag{3}$$

where  $u_k$  is the process noise, white Gaussian with zero mean, characterized by the covariance matrix  $Q_k$  and  $v_k$  is the measurements noise, white Gaussian with zero mean, characterized by the

<sup>4</sup> Asteroid Bennu and Itokawa were taken as a study cases

<sup>5</sup> These are the only celestial bodies that give a “relevant” contribution, although several order of magnitude lower than the other contributions.

<sup>6</sup> The reference frame used for the simulation is EME2000

<sup>7</sup> In the picture asteroid Bennu is represented as a sphere for simplicity

covariance matrix  $R_k$ . The filter is then completed with an equation that provides estimation of the covariance matrix associated with the estimation error, given by

$$P_{k+1}^- = \phi_k P_k \phi_k^T + Q_k. \tag{4}$$

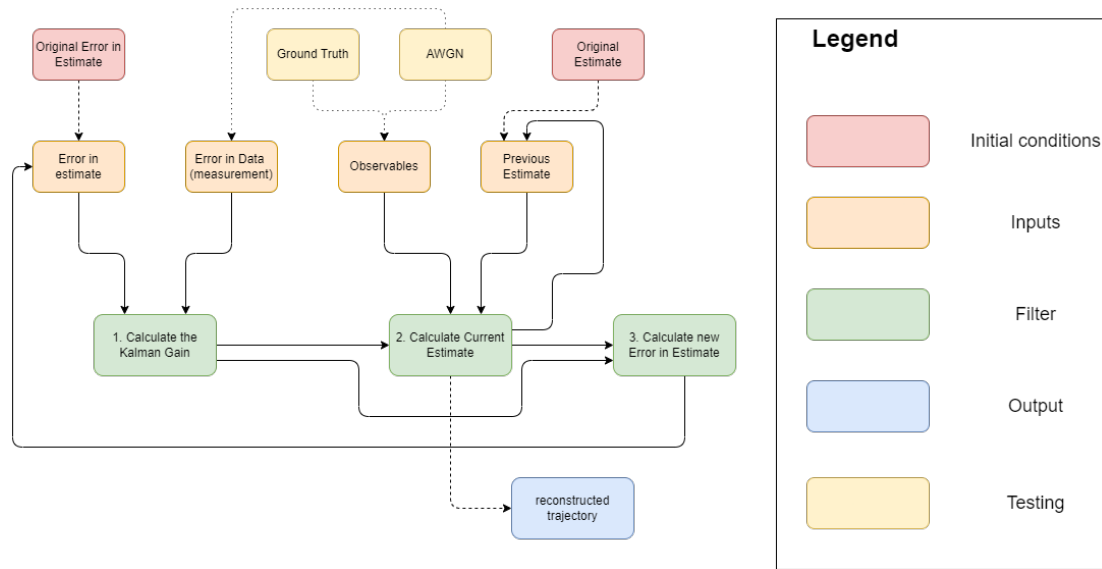


Figure 3: Flowchart of the Kalman Filter

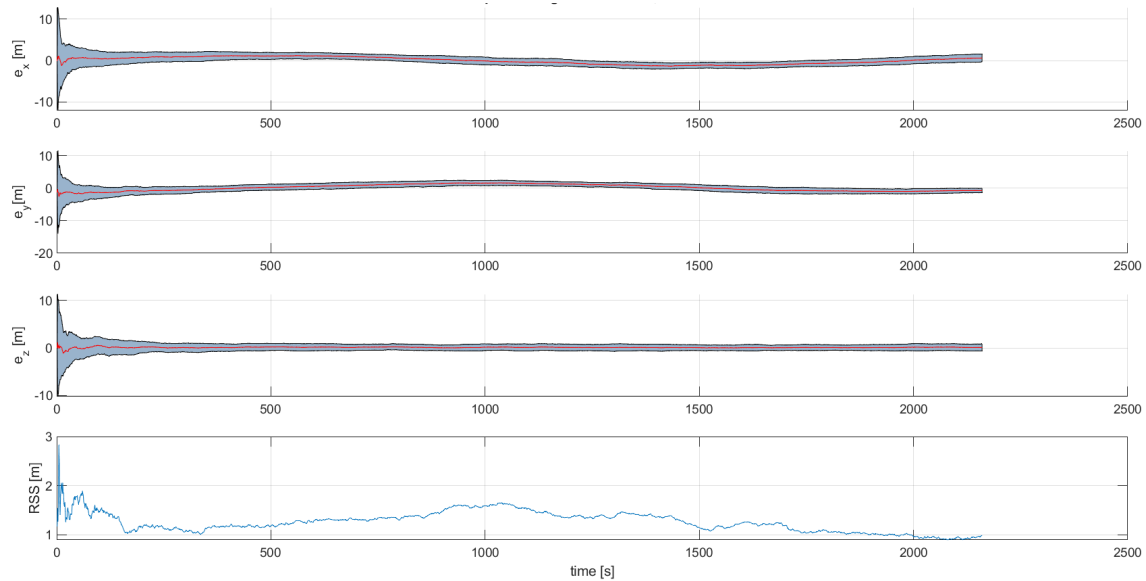


Figure 4: Error in trajectory reconstruction. From top to bottom, the error on the x, y and z axes and the quadratic sum of the RMS in the three coordinates.

In order to test the filter, a "ground truth" trajectory was generated using the dynamic model of the propagator, and it was used as a reference to compare with the reconstructed one generated by the filter. The synthetic observables that were fed to the filter were created from the "true" trajectory, adding white gaussian noise with different values of standard deviation and zero mean. Then, two different sets of Monte Carlo simulations were performed, the first one with different

values of the process noise covariance matrix, i.e.  $Q^{\delta}$ , in order to find the optimal value/s. These values were then used in the second simulation to test the filter performances. As can be seen in Figure 4, after a short initial transient, the filter is able to reconstruct the trajectory, minimizing the difference with the reference one.

### Design of the Navigation Computer

The Navigation computer (Figure 5 and Figure 6) was designed with the software Altium Designer, and is composed of the following elements:

- *Microcontroller*, STM32F407, a 32-bit ARM Cortex-M4 based device which is the core of the breadboard;
- *Connections*:
  - UART/USB protocols, used to communicate with the AI computer;
  - JTAG protocol, used to communicate with the Programmer (which is needed to upload the SW);
- *Memory*:
  - EEPROM;
- *Debug elements*:
  - LED, used to verify the correct functioning of the power alimentation and of the microcontroller;
  - Test pad, used to test the correct alimentation of some components of the breadboard.

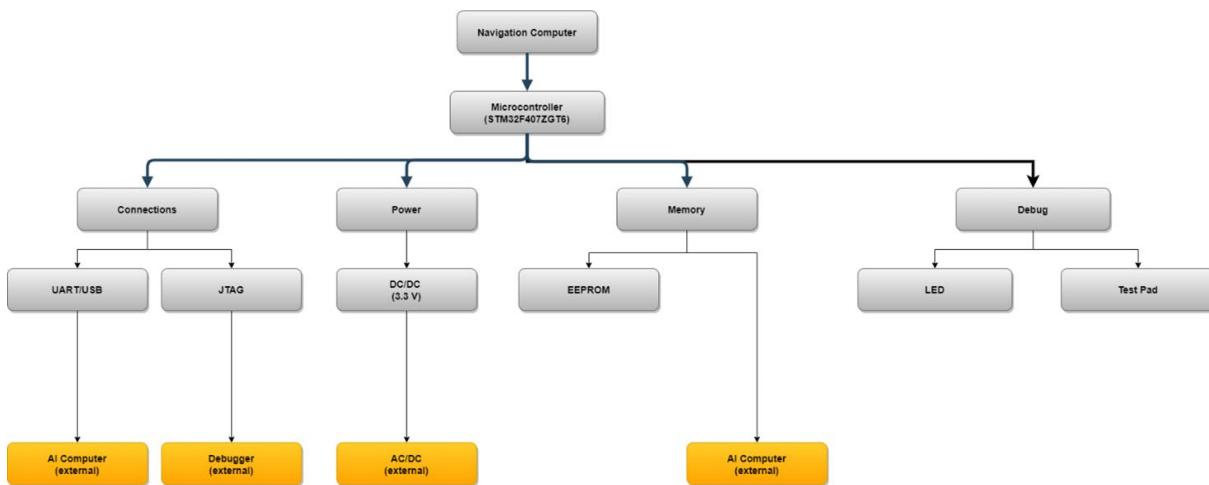


Figure 5: Tree structure of the navigation computer.

### Future work

The orbit determination simulator, together with the Extended Kalman Filter, will be integrated within the navigation computer, while the artificial intelligence algorithms will be implemented in a dedicated AI computer. Both of the aforementioned computers will be integrated into the same board and will have data interfaces that will allow internal data exchange between the two logic units and communication with the outside world. Specifically, the internal data exchange will mainly consist of sending information extracted from the images from the AI computer to the navigation computer. The latter will integrate this information with the dynamics of the system through an estimation filter, thus allowing the orbit of the CubeSat to be precisely estimated and

<sup>8</sup> The process noise covariance  $Q$  is a  $n \times n$  weighting matrix for the system process, where  $n$  is the number of state variables.

propagated over time. The last part of the project will consist in a campaign test to demonstrate the capabilities of the sub-system.

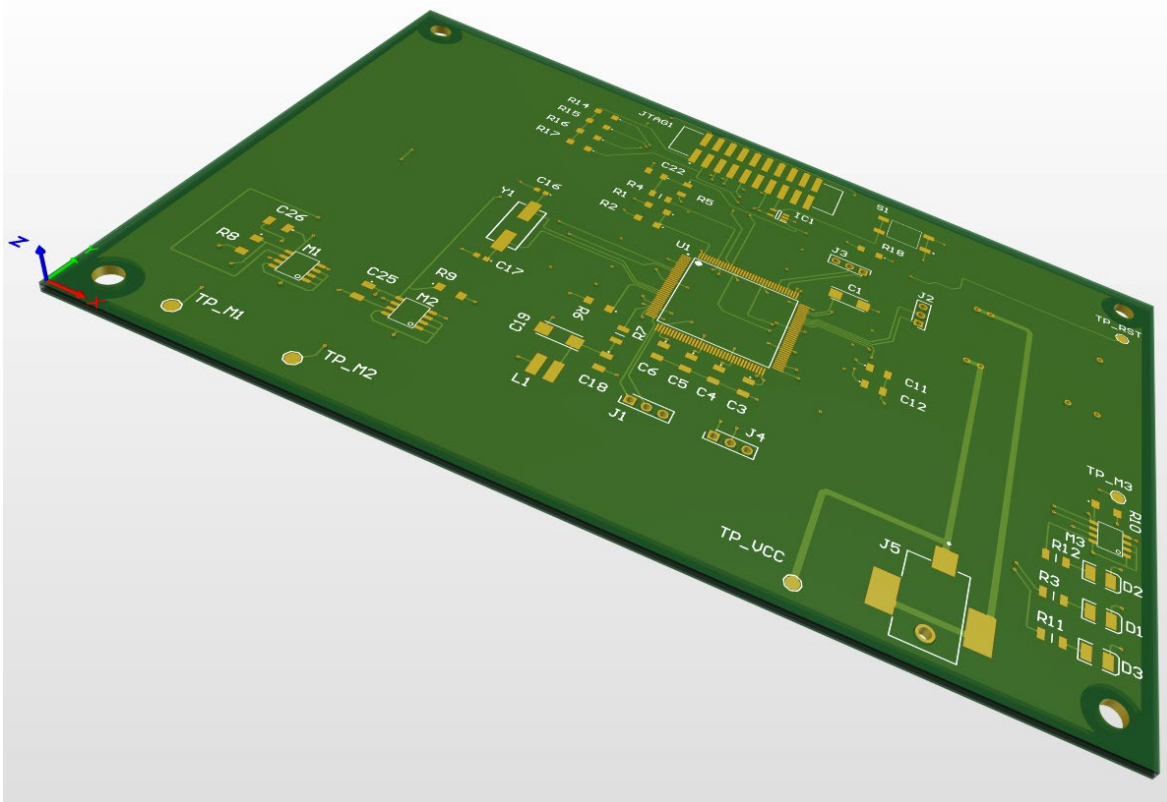


Figure 6: Design of the Navigation Computer. The PCB is composed of 4 layers, with the GND and PWR layers in the middle.

### Acknowledgment

The DeepNav (Deep Learning for Navigation of Small Satellites about Asteroids) project has been financed under ASI Contract N. 2021-16-E.0.

### References

- [1] R. Lasagni Manghi, M. Zannoni, and P. Tortora, An autonomous optical navigation filter for a CubeSat mission to a binary asteroid system, presented at the IEEE International Workshop on Metrology for AeroSpace, MetroAeroSpace, 2019, pp. 116-120.
- [2] E. Turan, S. Speretta, and E. Gill, Autonomous navigation for deep space small satellites: Scientific and technological advances, *Acta Astronautica*, vol. 193, pp. 56-74, Apr. 2022, doi: 10.1016/j.actaastro.2021.12.030. <https://doi.org/10.1016/j.actaastro.2021.12.030>
- [3] V. Franzese, F. Topputo, F. Ankersen, and R. Walker, Deep-Space Optical Navigation for M-ARGO Mission, *J Astronaut Sci*, vol. 68, no. 4, pp. 1034-1055, Dec. 2021, doi: 10.1007/s40295-021-00286-9. <https://doi.org/10.1007/s40295-021-00286-9>
- [4] E. Dotto et al., LICIAcube - The Light Italian Cubesat for Imaging of Asteroids In support of the NASA DART mission towards asteroid (65803) Didymos, *Planetary and Space Science*, vol. 199, p. 105185, May 2021, doi: 10.1016/j.pss.2021.105185. <https://doi.org/10.1016/j.pss.2021.105185>

- [5] R. Lasagni Manghi, D. Modenini, M. Zannoni, and P. Tortora, Measuring the mass of a main belt comet: Proteus mission, in Proceedings of the International Astronautical Congress, Oct. 2018. <https://doi.org/10.1109/MetroAeroSpace.2019.8869616>
- [6] E. Gramigna et al., Hera Inter-Satellite link Doppler characterization for Didymos Gravity Science experiments, presented at the 2022 IEEE 9th International Workshop on Metrology for AeroSpace, 2022, pp. 430-435. <https://doi.org/10.1109/MetroAeroSpace54187.2022.9856049>
- [7] C. Buonagura et al., Deep Learning for Navigation of Small Satellites about Asteroids: an Introduction to the DeepNav Project, presented at the 2nd International Conference on Applied Intelligence and Informatics, Sep. 2022. [https://doi.org/10.1007/978-3-031-25755-1\\_17](https://doi.org/10.1007/978-3-031-25755-1_17)
- [8] H. Demura et al., Pole and Global Shape of 25143 Itokawa, Science, vol. 312, no. 5778, pp. 1347-1349, Jun. 2006, doi: 10.1126/science.1126574. <https://doi.org/10.1126/science.1126574>
- [9] D. J. Scheeres et al., Heterogeneous mass distribution of the rubble-pile asteroid (101955) Bennu, Sci. Adv., vol. 6, no. 41, p. eabc3350, Oct. 2020, doi: 10.1126/sciadv.abc3350. <https://doi.org/10.1126/sciadv.abc3350>
- [10] D. J. Scheeres et al., The dynamic geophysical environment of (101955) Bennu based on OSIRIS-REx measurements, Nat Astron, vol. 3, no. 4, pp. 352-361, Mar. 2019, doi: 10.1038/s41550-019-0721-3. <https://doi.org/10.1038/s41550-019-0721-3>
- [11] D. A. Vallado and W. D. McClain, Fundamentals of astrodynamics and applications, 3. ed., 1. printing. Hawthorne, Calif.: Microcosm Press [u.a.], 2007. [https://doi.org/10.1016/S1874-9305\(07\)80003-3](https://doi.org/10.1016/S1874-9305(07)80003-3)
- [12] O. Montenbruck and E. Gill, Satellite orbits: models, methods, and applications: with ... 47 tables, 1. ed., corr. 3. printing. Berlin Heidelberg: Springer, 2005.
- [13] B. D. Tapley, B. E. Schutz, and G. H. Born, Statistical orbit determination. Amsterdam ; Boston: Elsevier Academic Press, 2004. <https://doi.org/10.1016/B978-012683630-1/50020-5>